Colloid and Interface Science Communications 49 (2022) 100645

Contents lists available at ScienceDirect

Colloid and Interface Science Communications

journal homepage: www.elsevier.com/locate/colcom

Rapid Communication

Influence of temperature and relative humidity on patterns formed in dried plasma and serum droplets

Leona Zurbriggen [a,b], Stephan Baumgartner [b,c,d], Nadine Schaub [e], Maria Olga Kokornaczyk [b,*]

[a] Faculty of Pharmaceutical Sciences, University of Basel, 4056 Basel, Switzerland
[b] Society for Cancer Research, 4144 Arlesheim, Switzerland
[c] Institute of Integrative Medicine, University of Witten-Herdecke, 58313 Herdecke, Germany
[d] Institute of Integrative and Complementary Medicine, University of Bern, 3010 Bern, Switzerland
[e] Medical Laboratory, Clinic Arlesheim, 4144 Arlesheim, Switzerland

ARTICLE INFO

Keywords:
Plasma
Serum
Desiccated droplets
Evaporation conditions
Pattern evaluation

ABSTRACT

In the present methodological study, we investigated the influence of different evaporation conditions upon patterns formed in desiccated plasma and serum droplets; furthermore, we determined the potential of such patterns to distinguish between four donors. Our results show that the development of different pattern features strongly depended on relative humidity: lower relative humidity triggered the formation of cracks, whereas higher relative humidity favored the development of inner crystalline structures. Settings that allowed for the best donor differentiation and at the same time showed high stability of the experimental system were 24.5 °C /15% rH and 30.5 °C /45% rH for plasma and 30.5 °C /15% rH and 36.6 °C /45% rH for serum droplets.

The results suggest that for the development of diagnostic tests based on pattern formation in evaporating plasma and serum droplets the choice of right evaporation conditions may influence the experimental system stability as also the test accuracy.

1. Introduction

Patterns emerging spontaneously in desiccating body fluids and their possible diagnostic applications have triggered the interest of scientists for a long time and have been investigated in a large number of studies [1]. The process of evaporation-induced pattern formation, being sensitive to even slightest changes in the composition of body fluids, may lead to the formation of patterns characterized by different morphologies able to reflect a donor's health status. For obtaining patterns, different methodological approaches have been developed, varying in the volume of the fluid to be evaporated, the way of its deposition on substrate, absence or addition of reagents, and, of course, the type of body fluid used itself [1]. Out of the different methodologies, the evaporation of undiluted body fluid droplets without addition of any reagent seems to represent the most frequently studied approach. Regarding the body fluids, saliva [2,3], tears [4–6], serum [7–9], blood [10–12], and plasma [7,13,14] have been studied most extensively. While evaporated saliva droplets, or smears, and tear droplets form the basis for recognized diagnostic tests used for the detection of the fertile period [15] and in the analysis of tear film quality [6], respectively, the use of desiccated blood and blood derivatives droplets for diagnostic purposes is still at a strictly experimental stage. We hypothesize a great potential of the latter regarding their diagnostic use for the detection of several systemic disorders, such as inflammation, diabetes mellitus, and cancer.

The process of droplet evaporation itself is well-known and has been addressed in many basic research studies regarding the evaporation of simple fluid droplets [16,17] or binary solution droplets [18,19]. Regarding basic research studies on the desiccation of biological fluids, there are some studies on the evaporation of full blood droplets [20–23], whereas other body fluids have been addressed in only a few or no publications [12,24,25]. Extant research has focused mainly on the influence of external factors (e.g. relative humidity, temperature, substrate type) upon phase transition and the resulting patterns obtained from body fluid collected from a single donor.

The present study investigated the influence of different temperature and relative humidity settings upon the pattern formation in drying plasma and serum droplets, and specified conditions that would favor the appearance of individual characteristics in the patterns obtained from fluid specimens collected from different donors. We assume that

* Corresponding author at: Society for Cancer Research, Kirschweg 9, 4144 Arlesheim, Switzerland.
E-mail address: m.kokornaczyk@vfk.ch (M.O. Kokornaczyk).

https://doi.org/10.1016/j.colcom.2022.100645
Received 3 May 2022; Received in revised form 4 July 2022; Accepted 5 July 2022
Available online 11 July 2022

such evaporation conditions might be optimal as well for further studies evaluating the accuracy of diagnostic tests using patterns obtained from dried plasma and serum droplets.

To the best of our knowledge, the present study is the first to analyze the influence of different settings of temperature and relative humidity upon the emerging patterns formed in desiccated plasma and serum droplets, and the potential to distinguish between specimens obtained from four different donors.

2. Materials and methods

2.1. Experimental design

In total, the experimentation consisted of 13 main experiments investigating the influence of relative humidity and temperature upon patterns from evaporated plasma and serum droplets, and three systematic control experiments for each fluid assessing the stability of the experimental system.

For the main experiments, serum and plasma specimens were collected from four apparently healthy volunteers. In addition to the droplet evaporation method (DEM), blood specimens obtained from the same volunteers were subjected to clinical chemistry analysis (Analytical Laboratory of the hospital *Clinic Arlesheim*; Arlesheim, Switzerland). The specimens obtained from a fifth volunteer were used for DEM systematic control experiments.

In the main DEM experiments, patterns from dried plasma and serum droplets were obtained under 13 different temperature and relative humidity settings. In each experiment, specimen samples from four donors were deposited on slides (3 plasma and 3 serum slides per donor, 10–16 droplets per slide) and placed in evaporation chambers following a quasi-randomization design.

Experimental system stability was assessed by means of systematic control experiments performed under temperature and relative humidity settings, which had allowed for the best differentiation between the four volunteers in the main experiments. In these experiments, plasma and serum specimens from the fifth volunteer were subjected to DEM analysis; evaluation followed the same quasi-randomization design as the corresponding main experiments.

The desiccated droplet residues were inspected by means of an optical microscope with an attached camera and photographed in dark- and bright-field in 25× magnification. The saved images were analyzed using the ImageJ software for several pattern evaluation parameters.

Statistical analysis of data generated in DEM and clinical chemistry analyses was performed with the software CoStat.

2.2. Specimen collection

Five apparently healthy volunteers were asked for a blood donation. Each volunteer signed a consent form for use of blood specimens for research; following donation, the blood specimens were anonymized.

Blood draw took place at the medical laboratory of the hospital *Clinic Arlesheim* (Arlesheim, Switzerland) in the morning. There were no specific instructions for the donors as to behavior before blood draw (e.g. fasting). The present project was not within the scope of the Swiss Human Research Act sect. 2, § 1, and did not require approval by an ethics committee.

For DEM analysis, blood from each volunteer was collected into one EDTA tube (for plasma) and one tube containing a serum separator and clot activator (for serum). The tubes were centrifuged (Centrifuge 5810, Eppendorf, Hamburg, Germany) at 2000 ×g for 15 min (EDTA tubes) or 10 min (tubes with serum separator). The plasma and serum specimens were then divided into 13 portions each. The portions were filled into Eppendorf tubes (Eppendorf Research Plus, Eppendorf, Hamburg, Germany), labeled, and stored at −21 °C until further analysis.

2.3. Main experiments

In total, 13 main experiments were performed under the following temperature/relative humidity settings: 18.5 °C/45%rH, 24.5 °C/15% rH, 24.5 °C/30%rH, 24.5 °C/45%rH, 30.5 °C/15%rH, 30.5 °C/30%rH, 30.5 °C/45%rH, 30.5 °C/60%rH, 36.6 °C/30%rH, 36.6 °C/45%rH, 36.6 °C/60%rH, 42.5 °C/30%rH, 42.5 °C/45%rH. In each setting, plasma and serum specimens obtained from the four volunteers were analyzed. For each type of fluid, three slides per volunteer were used with 10–16 droplets per slide.

2.4. Systematic control experiments

Systematic control experiments were set up exactly as the main experiments, but only analyzing specimens from one single volunteer. An absence of statistical differences in the systematic control experiments indicated that the experimental setup was robust.

Systematic control experiments were performed under three temperature/relative humidity settings for each fluid which had allowed for the best differentiation between the four donors in the main experiments (for plasma: 24.5 °C/30%rH, 30.5 °C/15%rH, 30.5 °C/45%rH and for serum: 30.5 °C/15%rH, 30.5 °C/45%rH and 36.6 °C/45%rH; Table 3). The choice of these settings was based on the outcome of a one-way analysis of variance with the factor “donor” performed on data from the main experiments. In particular, those settings were chosen which had reached highest significance levels in the main experiments (highest F and lowest p values) and which differentiated the samples collected from the four donors into at least three significance ranges.

In each systematic control experiment, four portions of a specimen obtained from one single volunteer were distributed over 12 microscope slides (each portion over 3 slides). The distribution of slides in the evaporation chamber followed the same quasi-randomization design as the corresponding main experiments.

Settings that (i) allowed for the best differentiation between the donors in the main experiments and (ii) showed either no significant differentiation between the control groups in the systematic control experiments, or featured a degree of significance much smaller than the one observed in the main experiments, were considered optimal for plasma and serum DEM experiments.

2.5. Droplet evaporation method

Slide preparation: microscope slides (76 × 26 mm, pre-cleaned, cut edges; Thermo Scientific, Gerhard Menzel B.V. & Co. KG, Braunschweig, Germany) were put into an ethanol 75% bath and following, into two purified water baths [26] (“purified water in bulk”, X-SEPTRON LINR 10 VAL, BWT AQUA AG, Aesch, Switzerland). Slides from the third bath were carefully wiped dry with a laboratory wiper (KIMTECH science, Kimberly-Clark Professional, Rosswell, Canada).

Droplet deposition: 1.6 µl plasma and serum droplets were deposited onto slides by means of a micro-pipette of 20 µl capacity (Eppendorf Research Plus, Eppendorf, Hamburg, Germany). 10–16 droplets (depending on the available specimen volume) were placed in two parallel rows.

Control and monitoring of evaporation conditions: droplet evaporation took place in a climatic exposure test cabinet (KBF 240, cooled incubator with controlled humidity system, WTB Binder Labortechnik GmbH, Tuttlingen, Germany) with temperature and relative humidity control. Inside the cabinet, two plexiglass inner chambers were placed and covered with semi-permeable foam. To monitor temperature and relative humidity conditions, sensors were placed inside the inner chambers (2 sensors), the cabinet (1 sensor), and in the laboratory (1 sensor). The sensors were connected to the computer, allowing for real-time monitoring. A humidifier was set up in the laboratory in order to match the conditions in which the droplets were deposited on slides as closely as possible to the conditions inside the climatic cabinet.

Deposition of slides inside the chambers: the slides with plasma droplets were placed in the lower inner chamber and the slides with serum droplets in the upper inner chamber. By placing the slides in the inner chambers, a quasi-randomized design was applied where slide allocation was randomized only within rows and not within columns.

2.6. Pattern acquisition

The dried droplets were photographed with an optical microscope (Zeiss Lab. A1; Carl Zeiss Microscopy GmbH, Jena, Germany) in magnification 25× with an attached camera (Moticam 5.0MP; CMOS; Motic Electric Group Co., Ltd., Xiamen, China). The scale-cross function of the Motic Image Plus 2.0 software was used to determine the exact center of the photographed area to allow for each dried droplet to be photographed in the same position. All droplet residues were photographed twice, in dark- and bright-field. The images were saved in JPG format and a size of 1360 × 1024 pixels.

2.7. Pattern evaluation

In the main experiments, a total of 3787 dark-field and 3768 bright-field images were analyzed using the software ImageJ 1.50b[27] with the GLCM-Texture plugin.[28] In the dark-field images, the texture parameter $entropy_{ROI}$ was determined, whereas in the bright-field images, the *crack total area* was measured.

For this purpose, a series of image transformations (Fig. 1) and measurements were performed.

As shown in Fig. 1(a-c), the dark-field images were transformed into 8-bit greyscale images and 500 × 500 pixel region of interests (ROIs) were cropped. To obtain the photographs, the droplets were positioned in a way that aligned their center with the geometrical center of the image. Correspondingly, the ROIs were set identically throughout the entire image database, ensuring that the points of intersection of the diagonals aligned with the image's geometrical center. Subsequently, by means of the plug-in GLCM Texture, the ROIs were subjected to the measurement of $entropy_{ROI}$.

On the bright-field images, a background subtraction (rolling ball = 75 pix, light background) and color threshold (by default method and hue-saturation-brightness color space with brightness setting 0–234) were performed in order to highlight the cracks. Images were converted into binary masks. Masks in which some other structures were visible beside the cracks were corrected by hand, deleting additional structures (Fig. 1d-f). Finally, by means of the particle analysis tool (particle size setting 25-infinity pix) the *crack total area* was measured.

2.8. Blood analyses

Analyses of the blood specimens collected from four volunteers were performed in the laboratory of the hospital *Clinic Arlesheim* (Arlesheim, Switzerland), measuring the following clinical chemistry parameters: sodium, potassium, calcium, chloride, phosphate, urea, creatinine serum, uric acid, TBIL/bilirubin, cholesterol, triglycerides, GLUCm/glucose, TP/total protein, albumin (with UniCel DxC 600i analyzer; Beckman Coulter Inc.) and sedimentation (manual sedimentation reading after 1 h of sedimentation in the Sedivette System; Starsted AG, Sevelen, Switzerland).

2.9. Statistical analysis

Statistical analysis was performed using the software CoStat (v. 6.4, CoHort Software). For evaluating the influence of relative humidity and temperature, the plasma and serum datasets were analyzed by means of a two-way analysis of variance (ANOVA) with two independent factors (temperature and relative humidity). For analyzing the differences between samples collected from different volunteers, a one-way ANOVA was performed on the datasets for each fluid and analysis day (with the factor "volunteer"). Both analyses were followed by post-hoc multiple mean comparison with LSD test.

In addition, the Bravais-Pearson linear coefficient of correlation r $(Cov(X,Y))/(SD(X)SD(Y))$ was computed to determine the degree of association between the DEM data and corresponding data of the blood analyses.

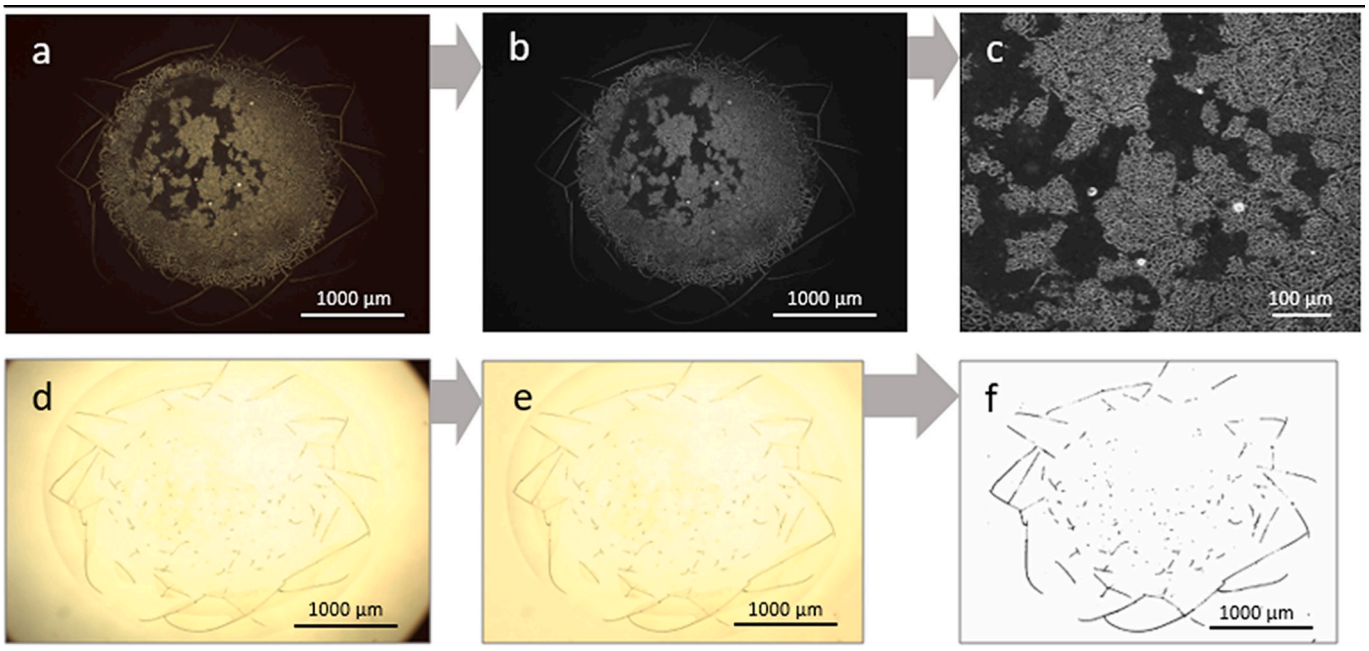

Fig. 1. Transformation steps performed on dark field images (a-c) and bright field images (d-f) for the calculation of the parameters $entropy_{ROI}$ and *crack total area*, respectively.

3. Results

3.1. Plasma and serum dried droplet patterns – General description

Examples of plasma and serum patterns obtained in the 13 examined temperature and relative humidity settings are shown in Fig. 2. Patterns obtained from both fluids resembled each other and contained two characteristic structure types: crystalline structures and cracks. While the crystalline structures were formed exclusively in the inner zone of the pattern, cracks predominantly appeared on the pattern's periphery.

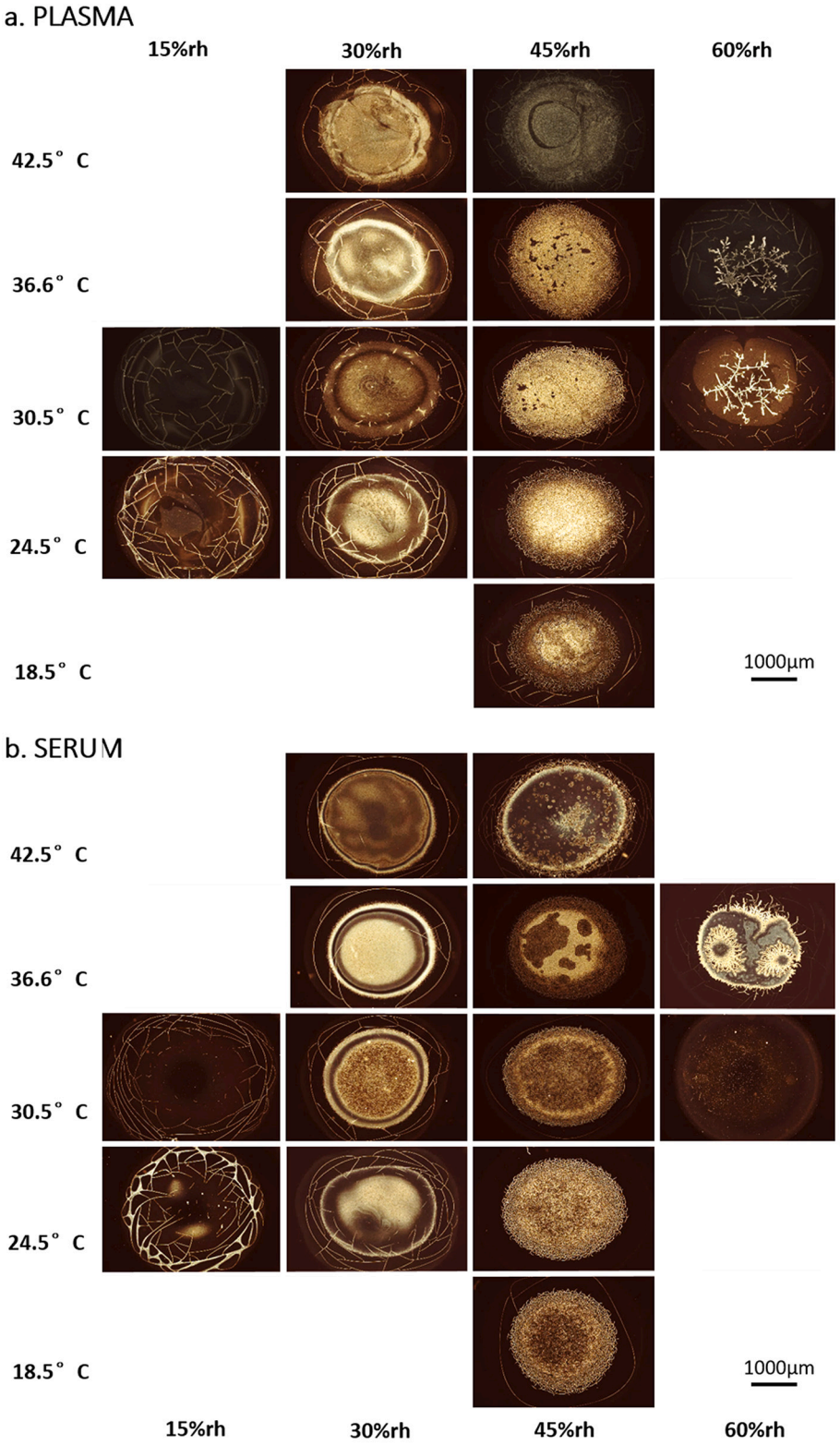

Fig. 2. Representative examples of droplet patterns of plasma (a) and serum (b) collected from one volunteer and evaporated in different temperature and relative humidity settings, photographed in dark-field in 25× magnification.

In most patterns, the border consisted of a thin line and was only barely visible.

With regard to the differences in patterns formed under different conditions, it was clearly visible that patterns formed at lower relative humidity levels contained more cracks, while those formed at higher relative humidity levels contained well-developed crystalline structures. Few patterns formed at the highest relative humidity level contained thick dendrites (ramified structures) in the central zone.

3.2. Influence of different relative humidity and temperature settings upon plasma and serum droplet patterns

The developmental degrees of the two main structure types visible in both plasma and serum dried droplets were assessed by means of two pattern evaluation parameters: (i) $entropy_{ROI}$ – characterizing the crystalline structures in the droplet center, and (ii) *crack total area* – characterizing the amount of cracks present predominantly in the droplet's peripheral zone. The relation of these two parameters to evaporation temperature and relative humidity for plasma and serum patterns are shown in Fig. 3.

In both plasma and serum patterns, the number of cracks decreased with the increase of relative humidity ($r = -0.98$ and $r = -0.93$, respectively), whereas $entropy_{ROI}$ increased steadily from 15%rH to 45% rH. The correlations between relative humidity and $entropy_{ROI}$ for plasma and serum patterns were $r = 0.33$ and $r = 0.85$, respectively.

The influence of temperature on both structure types found in dried plasma and serum droplets was much weaker than that of relative humidity. The correlations found between temperature and $entropy_{ROI}$ for plasma and serum amounted to $r = -0.30$ and $r = -0.43$, respectively, whereas those for cracks amounted to $r = 0.44$ and $r = 0.25$,

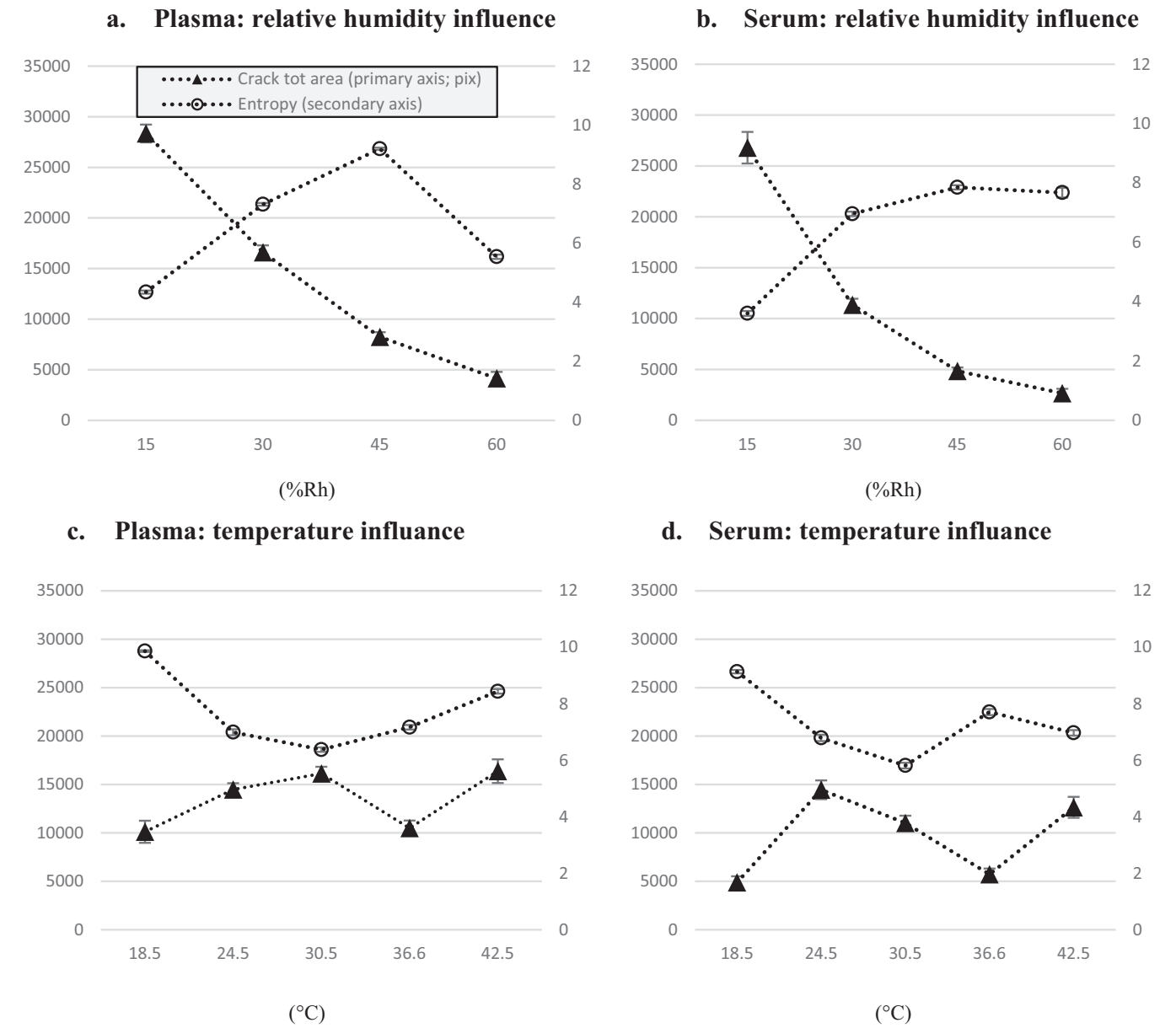

Fig. 3. Influence of relative humidity (a, b) and temperature (c, d) on the formation degree of cracks and inner crystalline structures assessed by the pattern evaluation parameters *crack total area* (triangles, mean ± standard error, principal axis (left), pixel) and $entropy_{ROI}$ (circles, mean ± standard error, secondary axis (right), unitless), respectively, in plasma and serum dry droplet patterns. The plotted temperature and relative humidity values were calculated from all images obtained in the main experimentation and are based on the entire relative humidity and temperature range, respectively (the values for $entropy_{ROI}$ were calculated from 3787 dark-field images and those of *crack total area* from 3768 bright-field images).

respectively.

The values of the F-distribution of a 3-way analysis of variance with the independent factors "relative humidity", "temperature", and "donor", indicating the ratio between the variation of the sample means and the variation within one sample, confirm the predominant influence of relative humidity upon plasma and serum patterns, especially for the pattern evaluation parameter *entropy$_{ROI}$* (4750.77 and 879.31, for plasma and serum, respectively) (Table 1). For the parameter *crack total area,* the influence of the factor "relative humidity" was similar to the influence of the factor "donor". The influence of temperature on both parameters was equal or smaller than that of the donor.

3.3. Optimal evaporation settings for plasma and serum droplets

Choosing the optimal evaporation settings for plasma and serum consisted of two steps. In the first step, those settings were determined in which the main experiments allowed for the best differentiation between the donors (highest F values and highest number of significantly different pair comparisons among the means in the 1-way analysis of variance with the factor "donor"). For plasma, the settings were: 24.5 °C/15%rH, 24.5 °C/30%rH, and 30.5 °C/45%rH, and for serum: 30.5 °C/15%rH, 30.5 °C/45%rH, and 36.6 °C/45%rH (Table 2, values in **bold**).

In the second step, systematic control experiments were performed at the chosen settings. Settings were considered optimal if the systematic control experiments showed no significant differences between the control groups, or the significance levels were much smaller than those observed in the main experiments. Settings in which the systematic control experiments showed large and significant differences between the control groups were not considered suitable. Following our study, optimal desiccation settings are 24.5 °C /15% rH and 30.5 °C /45% rH for plasma and 30.5 °C /15% rH and 36.6 °C /45% rH for serum droplets (Table 2, values marked with *).

3.4. Differentiation between the donors

As shown in Table 3, distinguishing between all donors was significant and possible by means of the parameter *entropy$_{ROI}$* of plasma droplets desiccated at 30.5 °C and 45%rH. Moreover, in both the optimal settings for serum droplets and the setting 24.5 °C/30%rH for plasma droplets, the parameter *entropy$_{ROI}$* differentiated three significant ranges between the donors. The parameter *crack total area* differentiated two significant ranges between the donors, with the exception of the setting 24.5 °C/30%rH for plasma droplets, where the differentiation of three ranges was possible.

Also visually, there were notable differences between the plasma and serum droplet patterns obtained from specimens collected from the four different volunteers (Fig. 4). Regarding the plasma patterns, specimens collected from volunteer 2 and 4 (called further samples 2 and 4) tended to form many cracks, while samples 1 and 3 formed fewer cracks. Regarding serum DEM patterns, sample 2 created the most cracks. Samples 2 and 4 created cracks extending into the central zone, whereas the cracks appearing in sample 1 and 3 were restricted to the peripheral zone. Regarding the crystalline structures formed in plasma patterns, samples 3 and 4 resembled each other in forming structures with a darker edge, while the structure became lighter towards the center. The light crystalline structure was divided by small gaps to form small angular platelet-shaped structures. Sample 1 showed a clear, dense structure, whereas the crystalline structure of sample 2 displayed features from all other samples. Additionally, the edge of the drop of sample 2 was surrounded by hair-like threads. The crystalline structures of serum samples resembled those found in plasma droplets. Nevertheless, in patterns of some serum samples, structure-free zones appeared. These void zones could cover almost the complete inner zone (sample 3) or only be confined to small spot-like areas (sample 4). Sample 1 showed a compact, platelet-shaped structure, with no structure-free zones. Sample 2 showed a dense structure with darker areas appearing inside the inner zone.

Table 1
F values of a 3-way analysis of variance with independent factors relative humidity, temperature, and donor for plasma and serum patterns from the 13 main experiments.

	F values – PLASMA		F values – SERUM	
	Entropy$_{ROI}$	*Crack total area*	*Entropy$_{ROI}$*	*Crack total area*
Relative humidity	4750.77	445.17	879.31	411.63
Temperature	119.72	46.89	156.99	14.09
Donor	225.31	490.84	105.15	481.27

Table 2
F values and number of donors (in brackets) that could be distinguished from each other (significant pairwise comparisons among the means of the four donors), determined in one-way ANOVA with the factor donor performed on image evaluation data sets of patterns formed in different temperature and relative humidity settings for plasma and serum. Settings that in the main experiments allowed for the best differentiation between the donors are marked in bold; settings in which systematic control experiments confirmed reasonable experimental system stability (see Table 3) are marked with "*".

F value (number of distinguished donors) – PLASMA					
		15 %RH	30 %RH	45 %RH	60 %RH
42.2 °C	*Entropy$_{ROI}$*		9.82 (2)	5.78 (2)	
	Crack area		24.67 (2)	36.71 (2)	
36.6 °C	*Entropy$_{ROI}$*		21.55 (3)	15.22 (2)	25.92 (3)
	Crack area		22.08 (3)	19.77 (2)	54.91 (2)
30.5 °C	*Entropy$_{ROI}$*	35.25 (3)	27.10 (3)	**72.21 (4)***	43.38 (3)
	Crack area	38.52 (2)	67.01 (2)	**311.89 (2)***	7.12 (2)
24.5 °C	*Entropy$_{ROI}$*	**134.01 (3)***	**118.73 (3)**	77.87 (3)	
	Crack area	**15.93 (2)***	**191.31 (3)**	31.40 (2)	
18.5 °C	*Entropy$_{ROI}$*			11.97 (3)	
	Crack area			293.13 (3)	
F value (number of distinguished donors) – SERUM					
42.2 °C	*Entropy$_{ROI}$*		21.97 (3)	70.42 (3)	
	Crack area		20.79 (2)	16.75 (2)	
36.6 °C	*Entropy$_{ROI}$*		27.72 (3)	**360.47 (3)***	6.45 (2)
	Crack area		16.01 (2)	**9.31 (2)***	27.87 (3)
30.5 °C	*Entropy$_{ROI}$*	**402.43 (3)***	87.61 (3)	**49.06 (4)**	22.88 (3)
	Crack area	**124.98 (2)***	38.01 (3)	**75.96 (2)**	15.85 (2)
24.5 °C	*Entropy$_{ROI}$*	14.55 (3)	14.91 (3)	32.58 (3)	
	Crack area	116.21 (2)	148.54 (2)	22.57 (2)	
18.5 °C	*Entropy$_{ROI}$*			23.23 (3)	
	Crack area			53.72 (2)	

3.5. Correlations between pattern evaluation parameters and blood analysis results

Table 4 presents the clinical chemistry readings and the correlations found between these parameters and the plasma and serum pattern evaluation parameters *entropy$_{ROI}$* and *crack total area,* both obtained from droplets desiccated in optimal conditions. For the settings with lower humidity favoring the formation of cracks, correlations between the clinical chemistry readings and *crack total area* were calculated, whereas correlations between the clinical chemistry readings and the crystalline structures (*entropy$_{ROI}$*) where calculated for settings with higher humidity, which were optimal for the development of these structures.

For plasma, *entropy$_{ROI}$* created strong correlations with potassium, creatinine serum, phosphate and total protein, whereas for serum no strong correlations could be identified. Regarding the image evaluation parameter *crack total area*, for plasma strong correlations could be found with glucose, triglycerides and bilirubin, whereas for serum it was glucose, triglycerides, bilirubin and calcium.

Table 3
Mean values of the pattern evaluation parameters *entropy$_{ROI}$* and *crack total area,* and *F* and *p* values of the 1-way analysis of variance of main and control experiments for plasma patterns. Different letters in brackets indicate significant differences at $p < 0.05$.

	n	*Entropy$_{ROI}$*	*n*	*Crack total area (*10^{-3})*	*n*	*Entropy$_{ROI}$*	*n*	*Crack total area (*10^{-3})*	*n*	*Entropy$_{ROI}$*	*n*	*Crack total area (*10^{-3})*
PLASMA	24.5 °C & 30%				30.5 °C & 15%				30.5 °C & 45%			
Volunteer 1	46	5.61 (c)	45	6.31 (c)	45	3.91 (b)	47	31.40 (b)	47	8.32 (d)	46	0.32 (b)
Volunteer 2	48	7.79 (b)	47	37.62 (a)	47	4.89 (a)	47	53.11 (a)	45	9.23 (b)	46	15.57 (a)
Volunteer 3	46	7.65 (b)	46	14.03 (b)	44	3.54 (c)	44	33.71 (b)	47	8.70 (c)	47	1.05 (b)
Volunteer 4	46	8.18 (a)	45	7.27 (c)	43	3.78 (bc)	46	32.47 (b)	47	9.40 (a)	45	0.53 (b)
F		118.73		191.31		35.25		38.52		72.21		311.79
p		0.0000 ***		0.0000 ***		0.0000 ***		0.0000 ***		0.0000 ***		0.0000 ***
F_{SCE}		1		10.81		15.35		0.17		1.11		24.45
p_{SCE}		0.3962 ns		0.0000 ***		0.0000 ***		0.9175 ns		0.3484 ns		0.0000 ***
SERUM	30.5 °C & 15%				30.5 °C & 45%				36.6 °C & 45%			
Volunteer 1	43	2.30 (c)	43	13.64 (b)	45	6.31 (c)	42	0.43 (b)	30	8.35 (a)	29	0.48 (b)
Volunteer 2	45	3.96 (a)	47	72.43 (a)	46	8.59 (a)	45	9.46 (a)	29	8.13 (a)	26	5.00 (a)
Volunteer 3	44	2.45 (b)	45	13.76 (b)	46	7.75 (b)	43	0.67 (b)	29	7.41 (b)	30	1.15 (b)
Volunteer 4	43	2.37(bc)	44	19.89(b)	46	5.41 (d)	45	0.65 (b)	30	4.34 (c)	29	3.46 (a)
F		402.43		124.98		49.06		73.96		360.47		9.31
p		0.0000 ***		0.0000 ***		0.0000 ***		0.0000 ***		0.0000 ***		0.0000 ***
F_{SCE}		2.24		2.62		144.03		8.34		0.98		1.32
p_{SCE}		0.0875 ns		0.0544 ns		0.0000 ***		0.0000 ***		0.4039 ns		0.2721 ns

LEGEND: SCE – systematic control experiment;

4. Discussion

The present study showed that both temperature and relative humidity influenced pattern formation in dried plasma and serum droplets. However, the influence of relative humidity was most pronounced. Both plasma and serum droplet patterns contained crystalline structures as well as cracks; at lower relative humidity levels, more cracks were formed and almost no crystalline structures, whereas at higher relative humidity levels, crystalline structures were well-developed and fewer cracks were formed. To understand this phenomenon, we refer to an investigation performed by Tarasevich and Pravoslavnova,[29] who studied the desiccation process of a complex fluid droplet (containing albumin and NaCl). According to this study, during the desiccation of a droplet a segregation process takes place in which salt particles get transported into the droplet center while albumin molecules remain more or less equally distributed. The higher salt concentration in the droplet center causes the appearance of crystalline structures, whereas in the droplet peripheral zone, the albumin by itself creates a film, and thus cracks may be formed. With regard to our present study it can be assumed that the evaporation process lasted longer at higher relative humidity levels and favored the occurrence of flows inside the droplet, thus transporting salts into the droplet center. Moreover, the prolonged evaporating time caused the droplet surface to dry slower and thus lesser internal tension to be built up, leading so to a reduced formation of cracks. In contrast, at lower relative humidity, quicker evaporation might reduce the segregation of salts, thus inhibiting the formation of crystalline structures. Fast evaporation might lead to a build-up of greater internal tension within the protein film, causing intense cracking of the surface.

The crystalline structures created at a relative humidity of 60% were composed of thick dendrites clearly organized in a centered structure, whereas those formed at lower relative humidity levels were characterized by a uniform formation of thin structures (Fig. 2). This difference may be caused by a higher and longer-lasting mobility of molecules due to the slower desiccation at 60%rH, and so the predominance of structure formation in course of diffusion limited aggregation[30] rather other structure-forming mechanisms.

Our study aimed to specify the evaporation conditions under which the differences in the plasma and serum patterns obtained from different donors would be greatest; however, it does not establish any connection between the observed differences and donor-related factors such as age, gender, life-style, blood group, or health condition. The connection between plasma and serum patterns and health conditions is crucial for a possible diagnostic application and has been addressed in a many studies [1]. Regarding other factors and their possible influence upon the patterns, knowledge is rather limited. Blood and blood derivative constituents are known to vary with age and between genders [31] which may thus reflect in dried droplet patterns; such connections should be examined in detail in further clinical studies. We assume that the evaporation conditions specified here may be recommended for future investigations.

We identified two optimal evaporation conditions for plasma (24.5 °C/30%rH, 30.5 °C/45%rH) and two for serum droplets (30.5 °C/15%rH, 36.6 °C/45%rH) allowing for best differentiation between the specimens obtained from different donors. For both fluids in the first setting, the cracks dominate, whereas in the second setting this applies to crystalline structures. In plasma, however, in the first setting (at 30% rH) crystalline structures were present as well. The degree of development of both structure types, measured by means of *crack total area* and *entropy$_{ROI}$*, correlated with certain parameters of the blood analyses. For both fluids, cracks correlated positively with glucose and triglycerides, and negatively with bilirubin, whereas the crystalline structures in serum droplets created correlations only in plasma, positive for creatinine serum and potassium, and negative for phosphates and total protein. Similar correlations have also been reported by other authors.[29,32] In the present study, the reliability of the correlations found must be questioned due to the small sample size and should be critically examined on a larger scale in further investigations.

Since the two pattern evaluation parameters *entropy$_{ROI}$* and *crack total area*, created different correlations with the blood constituents, it is clear that they also ranked the volunteers in different orders (Table 3). However, under the two specified optimal evaporation conditions, these pattern evaluation parameters ranked the volunteers in the same or at least very similar orders; with the exception of volunteer 1 who for serum droplets evaporated at 30.5 °C/15%Rh obtained the lowest *entropy$_{ROI}$* value (2.30) and the highest value for droplets evaporated at 36.6 °C/45%Rh (8.35). Such difference in rankings may reflect the influence of varying evaporation conditions on the development of patterns features.

It is evident that any correlations between different blood constituents and the degrees of development of the structure types found in dried plasma and serum droplets play a role when speculating about future diagnostic applications of the droplet evaporation method (DEM) for identifying certain target conditions. In such a case, for instance, the

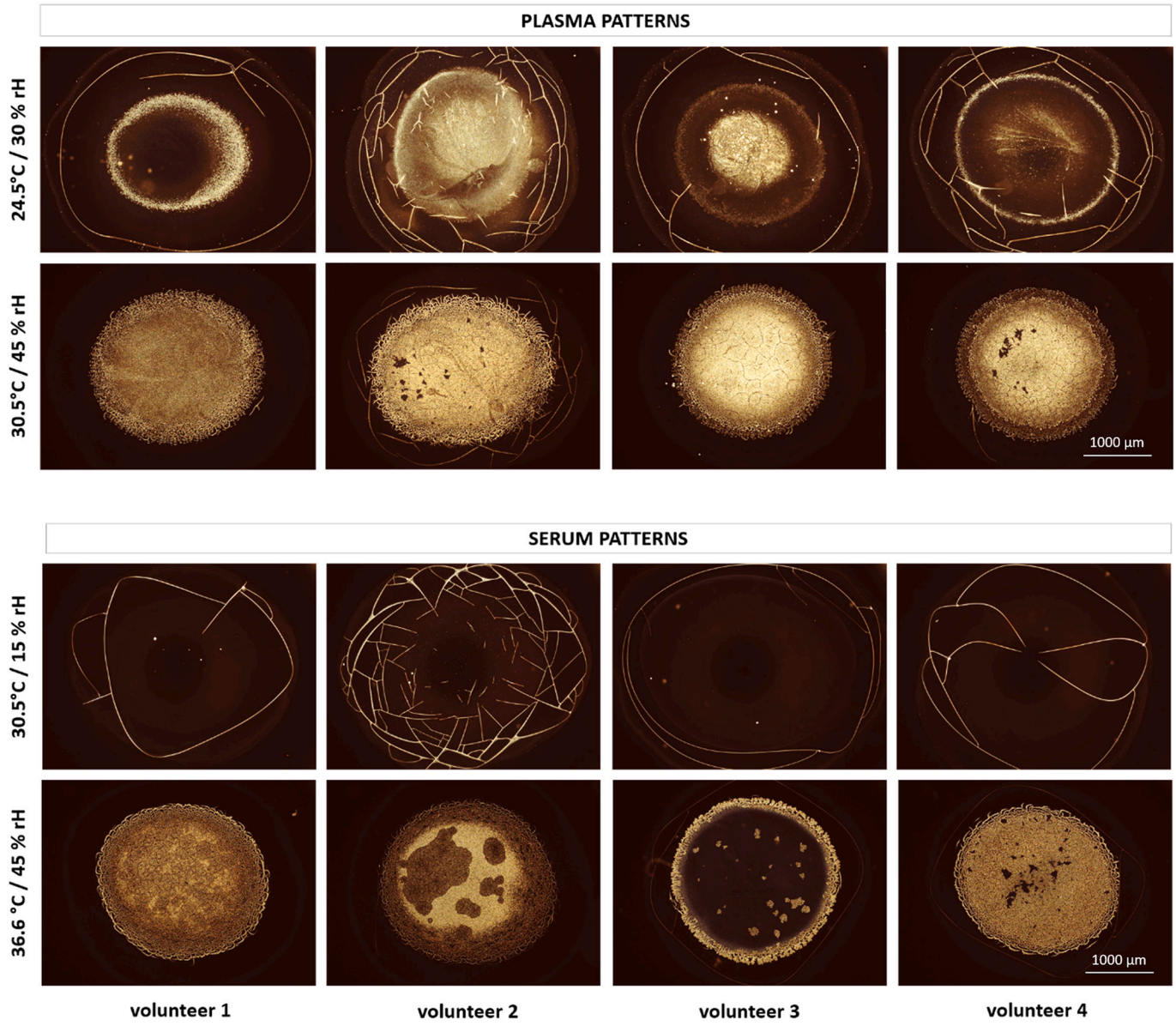

Fig. 4. Examples of patterns obtained from plasma and serum droplets desiccated in optimal conditions from samples collected from 4 apparently healthy donors. For the figure, images with $entropy_{ROI}$ values close to the mean value for the whole sample were chosen.

diagnosis of diabetes mellitus characterized by changed blood glucose levels might be aided by conditions favoring crack formation by setting drier evaporation conditions. On the other hand, diagnostic accuracy in the detection of kidney disorders might be augmented by drying plasma droplets at higher levels of relative humidity and subsequently analysis of crystalline structures, as this setup would be able to reflect variations in creatinine serum levels.

Further comparing the application of DEM to plasma and serum samples, our experiments showed that a delamination of the surface film made it difficult to obtain sharp photographs from plasma droplets. In case of serum droplets, the film did not delaminate and thus serum was easier to handle, especially during pattern acquisition. Moreover, results obtained from serum droplet analysis showed clearer differences between the donors. On the other hand, plasma droplet patterns created stronger and more reliable correlations with the blood analyses results. Further research should be carried out to understand the benefits and limitations of the application of DEM on both respective fluids for diagnostic purposes.

Since pattern formation in evaporating droplets is a highly sensitive process that can be easily influenced by condition gradients inside the climatic cabinet, we performed systematic control experiments in addition to the main experiments in order to test the experimental system stability [33]. The experimental design of the systematic control experiments was the same as that of the main experiments, except that instead of the four specimens collected from four different volunteers, here four portions of a single specimen (collected from the fifth volunteer) were compared. In a stable experimental system, there should be no statistically significant differences between the four portions of this single specimen. As shown in Table 3, four out of six systematic control experiments performed under the same evaporation conditions as the corresponding main experiments showed no or, in comparison to the main experiments, only minor statistical differences, indicating that the experimental system was stable under these conditions. It can be noted that the pattern evaluation parameter $entropy_{ROI}$ was insignificant in all of these four experiments, whereas *crack total area* showed minor differences. The two other systematic control experiments performed at 30.5 °C/15%Rh for plasma and 30.5 °C/45%Rh for serum showed differences with greater significance, indicating the experimental system to

Table 4
Clinical chemistry blood parameters of the four volunteers (a) and correlations between these parameters and image evaluation parameters *entropy$_{ROI}$* (for conditions with higher relative humidity values favoring the formation of inner crystalline structures) and *crack total area* (for conditions with lower relative humidity values favoring the formation of cracks) for patterns in plasma and serum droplets desiccated in optimal conditions (b). For each correlation a correlation coefficients (r) is given; values <-0.85 and >0.85 (indicating strong negative and positive correlations, respectively) are in **bold**.

a. **Clinical chemistry blood parameters**

Parameter / reference values	**Volunteer 1**	**Volunteer 2**	**Volunteer 3**	**Volunteer 4**
Sodium [mmol/L] / 136–145	136	137	140	139
Potassium [mmol/L] / 3.5–5.1	3.9	4.2	3.9	4.2
Calcium [mmol/L] / 2.15–2.55	2.25	2.24	2.26	2.26
Chloride [mmol/L] / 98–107	99	100	102	102
Phosphate [mmol/L] / 0.87–1.45	1.31	0.94	1.1	0.94
Urea [mmol/L] / <8.3	2.9	6.4	6.5	6.1
Creatinine serum [µmol/L] / 44–106	63	73	72	74
Uric acid [µmol/L] / 155–428	274	331	342	251
TBIL/bilirubin [µmol/L] / ≤17.1	14.8	12.2	14.8	14
Cholesterol [mmol/L] / <5.0	6.22	5.88	4.82	5.97
Triglycerides [mmol/L] / <2.3	1.6	3.35	1.33	0.83
GLUCm/glucose [mmol/L] / 4.1–8.0	5.25	8.64	5.77	5.23
TP/total protein [g/L] / 64–83	78	75	75	74
Albumin [g/L] / 35–52	45	44	47	45
Sedimentation reaction [mm/h] / ≤10	10	4	5	6

b. **Correlations between the clinical chemistry blood parameters and image evaluation parameters**

	Plasma		**Serum**	
	Entropy$_{ROI}$	*Crack total area*	*Entropy$_{ROI}$*	*Crack total area*
	30.5 °C / 45%rH	**24.5 °C / 30%rH**	**36.6 °C / 45%rH**	**30.5 °C / 15%rH**
Sodium	0.34	−0.19	−0.56	−0.33
Potassium	**0.94**	0.48	−0.51	0.66
Calcium	−0.03	−0.78	−0.64	**−0.84**
Chloride	0.51	−0.19	−0.72	−0.28
Phosphate	**−0.97**	−0.53	0.55	−0.57
Urea	0.74	0.49	−0.38	0.40
Creatinine serum	**0.88**	0.42	−0.57	0.39
Uric acid	−0.12	0.66	0.60	0.41
Bilirubin	−0.67	**−0.90**	−0.09	**−0.98**
Cholesterol	0.07	−0.07	−0.05	0.20
Triglycerides	0.15	**0.93**	0.63	**0.92**
Glucose	0.39	**0.99**	0.43	**0.97**
Total protein	**−0.88**	−0.28	0.68	−0.26
Albumin	−0.40	−0.47	−0.05	−0.70
Sedimentation reaction	−0.71	−0.19	0.18	−0.60

be unstable under these specific conditions. This result points to yet unidentified external influences on pattern formation present in the experiments, which need to be investigated, identified, and controlled in future investigations.

In several studies regarding DEM as a possible diagnostic test applied on blood and blood derivatives, the given temperature and relative humidity conditions during evaporation were not specified, or the evaporation occurred under ambient conditions lacking control and/or monitoring [1,12]. Based on the results of the present study it can be claimed that the conditions under which evaporation takes place have an immense impact on pattern features and may also influence any diagnostic test result. Therefore, the evaporation conditions should be carefully chosen, controlled during the experiment, and finally stated along with the test result.

5. Outlook

The study presented here suggests a decisive impact of evaporation conditions upon the characteristics of the emerging patterns in dried droplets obtained from plasma or serum. Furthermore, it shows that the pattern characteristics formed under different evaporation conditions correlate with different blood constituents. These observations lead us to the hypothesis that DEM's sensitivity when applied as a diagnostic test for target conditions characterized by quantitative changes of certain blood constituents (e.g. diabetes mellitus characterized by elevated glucose, or kidney disorders characterized by elevated creatinine serum levels) might be enhanced or diminished by evaporation conditions impacting the formation of structures related to the blood constituents affected by the disease. The relation between the diagnostic test sensitivity towards different target conditions and the temperature and relative humidity settings applied during droplet evaporation should be investigated in clinical studies with well-defined patient groups.

Author declaration

There is no conflict of interest.

CRediT authorship contribution statement

Leona Zurbriggen: Conceptualization, Methodology, Investigation, Resources, Writing – original draft. **Stephan Baumgartner:** Conceptualization, Project administration, Writing – review & editing. **Nadine Schaub:** Resources, Investigation, Writing – review & editing. **Maria Olga Kokornaczyk:** Conceptualization, Methodology, Investigation, Resources, Data curation, Writing – original draft, Writing – review & editing, Supervision.

Declaration of Competing Interest

None.

Data availability

Data will be made available on request.

References

[1] M.O. Kokornaczyk, N.B. Bodrova, S. Baumgartner, Diagnostic tests based on pattern formation in drying body fluids - a mapping review, Colloids Surf. B: Biointerfaces 208 (2021), 112092.
[2] A.K. Martusevich, V.A. Yanchenko, O.B. Zhdanova, F. Artese, L.A. Napisanova, R. Virbalene, Crystallization characteristics of biological fluids of patients with postoperative alveococcosis, Clin. Med. 6 (2014) 38–42.
[3] I. Spinei, O. Balteanu, A. Spinei, E. Stepco, Crystallogenesis of oral fluid in the diagnosis of dental caries and inflammatory periodontal diseases in children, in: Proceedings of the 4th IEEE International Conference on E-Health and Bioengineering, 2013, p. 2013. Iasi, Romania, November 21-23.

[4] M. Nebbioso, M. Sacchetti, G. Bianchi, A.M. Zicari, M. Duse, P. del Regno, A. Lambiase, Tear ferning test and pathological effects on ocular surface before and after topical cyclosporine in vernal keratoconjunctivitis patients, J. Ophthalmol. 2018 (2018 Oct 14), 1061276, https://doi.org/10.1155/2018/1061276. PMID: 30405906; PMCID: PMC6204206.
[5] A.M. Masmali, Y.A. Maeni, G.A. El-Hiti, P.J. Murphy, T. Almubrad, Investigation of ocular tear ferning in controlled and uncontrolled diabetic subjects, Eye Contact Lens 44 (2018) 70–75.
[6] A.M. Masmali, C. Purslow, P.J. Murphy, The tear ferning test: a simple clinical technique to evaluate the ocular tear film, Clin. Exp. Optom. 97 (2014) 399–406.
[7] T.A. Yakhno, V.G. Yakhno, A.G. Sanin, O.A. Sanina, A.S. Pelyushenko, N. A. Egorova, I.G. Terentiev, S.V. Smetanina, O.V. Korochkina, E.V. Yashukova, The informative-capacity phenomenon of drying drops, IEEE Eng. Med. Biol. Mag. 96-104 (2005).
[8] B.N. Levitan, A.R. Umerova, D.M. Abjalilova, A.K. Ayupova, The types of blood serum structural organization in chronic hepatitis and liver cirrhosis, Astrakhan Med. J. 5 (2010) 94–97.
[9] A.A. Killeen, N. Ossina, R.C. McGlennen, S. Minnerath, J. Borgos, V. Alexandrov, Protein self-organization patterns in dried serum reveal changes in B-cell disorders, Mol. Diag. Ther. 10 (2006) 371–380.
[10] L. Hamadeh, S. Imran, M. Bencsik, G.R. Sharpe, M.A. Johnson, D.J. Fairhurst, Machine learning analysis for quantitative discrimination of dried blood droplets, Sci. Rep. 10 (2020) 3313.
[11] L. Bahmani, M. Neysari, M. Maleki, The study of drying and pattern formation of whole human blood drops and the effect of thalassaemia and neonatal jaundice on the patterns, Colloids Surf. A Physicochem. Eng. Asp. 513 (2017) 66–75.
[12] R. Chen, L. Zhang, D. Zang, W. Shen, Blood drop patterns: formation and applications, Adv. Colloid Interf. Sci. 231 (2016) 1–14.
[13] E. Rapis, A change in the physical state of a nonequilibrium blood plasma protein film in patients with carcinoma, Tech. Phys. 47 (2002) 510–512.
[14] A. Brzecki, A. Brzecka, E. Gruszka, P. Olejniczak, M. Cyrul, Dry drop blood plasma - a new approach in the diagnosis of neoplastic diseases, Mater. Med. Pol. 3 (1998) 170–174.
[15] U.F.D. Administration, Ovulation (Saliva Test), 2018.
[16] R.D. Deegan, O. Bakajin, T.F. Dupont, G. Huber, S.R. Nagel, T.A. Witten, Contact line deposits in an evaporating drop, Phys. Rev. E Stat. Phys. Plasmas Fluids Relat. Interdiscip. Topics 62 (2000) 756–765.
[17] M. Budakli, Prediction of maximum spreading factor after drop impact: Development of a novel semi-analytical model incorporating effect of surface roughness, Colloids Interface Sci. Commun. 41 (2021) 100384. ISSN 2215-0382, https://doi.org/10.1016/j.colcom.2021.100384.
[18] R.D. Deegan, Pattern formation in drying drops, Phys. Rev. E Stat. Phys. Plasmas Fluids Relat. Interdiscip. Topics 61 (2000) 475–485.
[19] A.W. Zaibudeen, S. Khawas, S. Srivastava, Understanding multiscale assembly mechanism in evaporative droplet of gold nanorods, Colloids Interface Sci. Commun. 44 (2021) 100492. ISSN 2215-0382, https://doi.org/10.1016/j.colcom.2021.100492.
[20] W. Bou Zeid, D. Brutin, Influence of relative humidity on spreading, pattern formation and adhesion of a drying drop of whole blood, Colloids Surf. A Physicochem. Eng. Asp. 430 (2013) 1–7.
[21] D. Brutin, B. Sobac, B. Loquet, J. Sampol, Pattern formation in drying drops of blood, J. Fluid Mech. 667 (2011) 85–95.
[22] D. Brutin, B. Sobac, C. Nicloux, Influance of substrate nature on the evaporation of a sessile drop of blood, J. Heat Transf. 134 (2012) 0611011–0611017.
[23] B. Sobac, D. Brutin, Desiccation of a sessile drop of blood: cracks, folds formation and delamination, Colloids Surf. A Physicochem. Eng. Asp. 448 (2014) 34–44.
[24] J.M. Cameron, H.J. Butler, D.S. Palmer, M.J. Baker, Biofluid spectroscopic disease diagnostics: a review on the processes and spectral impact of drying, J. Biophotonics 11 (2018), e201700299.
[25] R. Chen, L. Zhang, W. Shen, Controlling the contact angle of biological sessile drops for study of their desiccated cracking patterns, J. Mater. Chem. B 6 (2018) 5867–5875.
[26] European Pharmacopoeia EDQM, Stasbourg, Council of Europe, France, 2020.
[27] C.A. Schneider, W.S. Rasband, K.W. Eliceiri, NIH image to ImageJ: 25 years of image analysis, Nat. Methods 9 (2012) 671–675.
[28] J. Cabrera, GLCM Texture Analyzer. https://imagej.nih.gov/ij/plugins/texture.html, 2003–2006.
[29] Y. Tarasevich, D. Pravoslavnova, Segregation in desiccated sessile drops of biological fluids, Eur. Phys. J. E Soft Matter. 22 (2007) 311–314.
[30] P. Meakin, Formation of fractal clusters and networks by irreversible diffusion-limited aggregation, Phys. Rev. Lett. 51 (1983) 1119–1122.
[31] L.V. Bel'skaya, E.A. Sarf, V.K. Kosenok, Age and gender characteristics of the biochemical composition of saliva: correlations with the composition of blood plasma, J. Oral Biol. Craniofac. Res. 10 (2020) 59–65.
[32] C. Ruoyang, L. Zhang, D. Zang, W. Shen, Understanding desiccation patterns of blood sessile drops, J. Mater. Chem. B 5 (2017) 8991–8998.
[33] M.O. Kokornaczyk, S. Wurtenberger, S. Baumgartner, Impact of succussion on pharmaceutical preparations analyzed by means of patterns from evaporated droplets, Sci. Rep. 10 (2020) 570.